Bull Eng Geol Environ (2017) 76:39–57
DOI 10.1007/s10064-016-0946-7

ORIGINAL PAPER

Refinement of categorization and scaling of weathering-related damage to natural stone: case study on oolitic limestone from El-Shatbi Tombs (Egypt)

G. M. E. Kamh[1] · S. Koltuk[2] · Hosam Ismael[3]

Received: 16 December 2014 / Accepted: 19 September 2016 / Published online: 14 November 2016

Abstract Natural rocks, as well as artificial building materials, in coastal regions are subject to severe attack by salts, primarily from sea spray, acid rain and/or domestic water in industrial and highly populated cities. As the oolitic limestone is the main rock through which the Greco-Roman sites had been excavated, then, the main aims of the current study are to define the damage category (DC) for the weathered oolitic limestone bedrock at coastal regions, with the Greco-Roman El-Shatbi Tombs serving as a case study. Additionally, it aims to modify the DC scale of Fitzner and Heinrichs (The Karolinum Press, pp. 11–56, 2002) to be applicable for defining the damage categories for a given archaeological site where the existing scale isn't based on any numerical limitations to previously define the DC of a given archaeological site. Detailed field investigations including photo-documentation, measurement of the dimensions of these weathering forms and consideration of the wall side orientation to sea spray at El-Shatbi Tombs have been used in tandem with the modified damage category scale to assess the damage category at these tombs. The net result of processing the field data indicated very severe damage at this site. The laboratory analysis for the small rock samples collected at El-Shatbi Tombs indicated that salts act within the pores of this limestone, particularly in 0.01–0.1-μm pores, at this semi-arid region.

Keywords Oolitic limestone · Weathering study · Damage category scale

✉ G. M. E. Kamh
g_kamh2000@yahoo.com

Hosam Ismael
hosam.ismael@artnv.au.edu.eg

[1] Geology Dept., Fac. of Sci., Menoufiya Univ, Shebin Al-Kom, Egypt

[2] LIH, RWTH Aachen Univ, Aachen, Germany

[3] Geography and GIS Dept., Fac. of Arts, Assiut Univ., New Valley Branch, Assiut, Egypt

Introduction

Weathering processes act on all sub-aerial materials with rates and intensities determined by many parameters, including the type of material and its weathering susceptibility, the number and intensity of the weathering cycles, and the specific processes prevailing at a given area (Takahashi et al. 1994; Kamh 2009a, b). The wall side orientation, tilting angle from vertical, rock surface roughness, and rock grain size affect the rock's weathering susceptibility (Attewell and Taylor 1990; Vendrell et al. 1996; Kamh and Azzam 2008). The rock and pore properties control the transport of salt solutions through the rock, as well as the rock's susceptibility to weathering, particularly to salts (McGreevy 1996; Flatt 2002; Török and Přikryl 2010; Yu and Oguchi 2010). The damage category [as indicated by the Fitzner and Heinrichs (2002) classification] starting from zero for buildings with no damage (i.e., the stone surface doesn't present any damage affecting its inscriptions and/or paints) to category 5 for buildings with very severe damage (i.e., totally damaged including its original historical inscriptions and/or paints).

Sea spray is one of the most prominent salt sources in coastal regions, affecting both recent and ancient structures as well as rock outcrops (Smith et al. 1994). Chloride and sulphate salts in sea spray physically disintegrate (through crystallization and/or hydration-dehydration pressure) the rocks' fabric, especially sedimentary rocks, e.g., sandstone

and limestone (Sperling and Cooke 1985). Such salts are the culprit behind most of the rock's weathering phenomena at a given building and/or archaeological site (Smith et al. 1994; Takahashi et al. 1994; Turkington 1998). The diagnostic salt weathering forms that can be recorded on a given rock are unlimited, including rock meal, exfoliation, scaling, honeycomb and tafoni, salt efflorescence, salt sub-florescence and surface disintegration (Smith and McGreevy 1983; McGreevy 1988; Smith et al. 1994; Smith and Přikryl 2007). These forms are defined based on Smith and McGreevy (1983) as listed in Table 1.

The extent of the damage caused by salts on a given rock can reach severe or very severe levels and can be defined using Fitzner and Heinrichs' (2002) classification as a non-destructive (descriptive and visually evaluated) technique. However, as this classification is not based on the weathering forms' dimensions, it has been modified in the current study to be applicable to and precisely define the damage category for a given rock mass, particularly at a given archaeological site.

Alexandria City, including El-Shatbi Tombs, is located on the coast of the Mediterranean Sea (Fig. 1). It is 40 km long, with a maximum width of 3 km inland from the seashore. It is bounded by latitudes 31°16′09″N and 31°22′28″N, and longitudes 28°40′12″E and 28°50′10″E (Fig. 1). Alexandria City is classified as a semi-arid region based on its pre-dominant climatic conditions listed in Table 2. The averages of minimum and maximum temperatures and relative humidity at Alexandria confirm a suitability for salt hydration/de-hydration particularly for sulfates (Zehnder and Schoch 2009). Alexandria City has been used, particularly El-Shatbi Tombs, as a case study as it represents a major sector of weathered Greco-Roman archaeological sites spread along the northern coast of

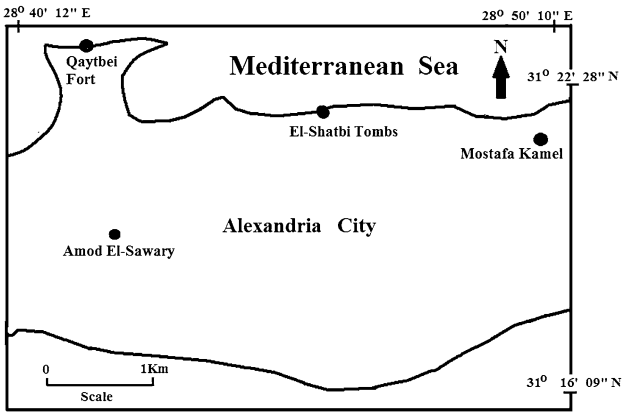

Fig. 1 Map of Alexandria City with its archaeological sites

Egypt's western desert. El-Shatbi Tombs, at latitude 31°22′02″N and longitude 28°45′30″E, have also been selected in the current study as they are affected by a wide range of weathering forms and damage categories, on their main bulk rock mass and inscriptions, as are all of the Greco-Roman sites in the Mediterranean region.

The Pleistocene Oolitic limestone ridges arranged in a descending order of age and height in the seaward direction are considered in the current study as the Greco-Roman archaeological sites, including the El-Shatbi Tombs; they have been excavated or built from these ridges. These ridges are parallel to and very close to the Mediterranean Sea coast and separated from one another by elongated depressions (Said 1990). Such limestone is chemically deposited in shallow marine agitated environments and forms singly to multiply laminated carbonate lamellae around siliceous or carbonate nuclei (Dunham 1962). These tombs are in contact with and at the base level of modern multi-storey buildings (Fig. 2b). The El-Shatbi

Table 1 Definition of weathering forms according to Smith and McGreevy (1983)

Weathering form	Definition
Rock meal	Is an alteration of a stone surface from coherent material into loose friable grains from coarse sand size to very fine powder
Exfoliation	Is separation of thin sheets, of few mm thick, of a stone's surface from the remaining mass of building blocks. These sheets are parallel to the stone's fabric
Scaling	Is separation of thin sheets, of few mm thick, of a stone's surface from the remaining mass of building blocks. These sheets are NOT parallel to the stone's fabric
Honeycomb	Is caverns formed by salt weathering at the stone's surface; these are of small diameter and depth, i.e., less than 0.5 m in dimensions
Tafoni	Is caverns formed by salt weathering at the stone's surface; these are of small diameter and depth, i.e., more than 0.5 m in dimensions
Salt efflorescence	Is a crystallization of salts at the stone's surface in a white color that alters to a dark color on dirt and pollutants' deposition from aerosols
Salt sub-florescence	Is an accumulation of salts in a sheet form below an impervious stone's surface resulting in scaling or exfoliation
Stone surface disintegration	Is separation of a stone's surface into small pieces due to stresses created by salts along the weak paths at this surface

Table 2 Climatic conditions at Alexandria City for the twenty years 1993–2013 (Egyptian Meteorological Authority)

Season	Average max. temp. °C	Average min. temp. °C	Range of relative humidity (%)	Range of rainfall (mm/year)
Summer	34	23	40–52	140–190
Winter	20	14	70–75	

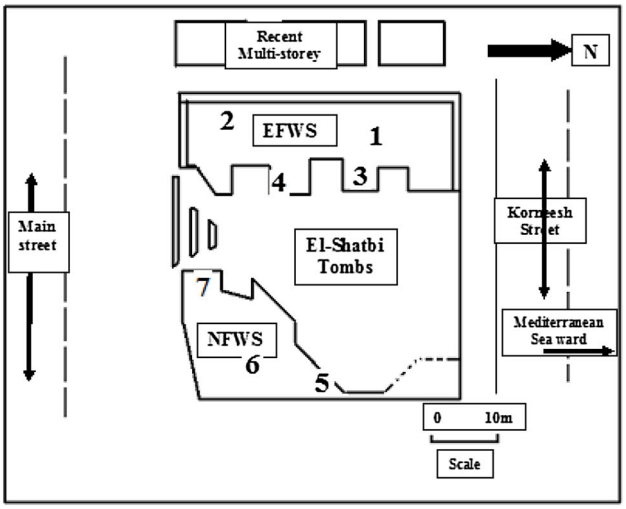

Fig. 2 Sketch of El-Shatbi tombs presenting its structure, wall side geographic orientation and location of the collected rock samples (**a**), and general view of the El-Shatbi Tombs and surrounding recent buildings (**b**), Alexandria City, Egypt

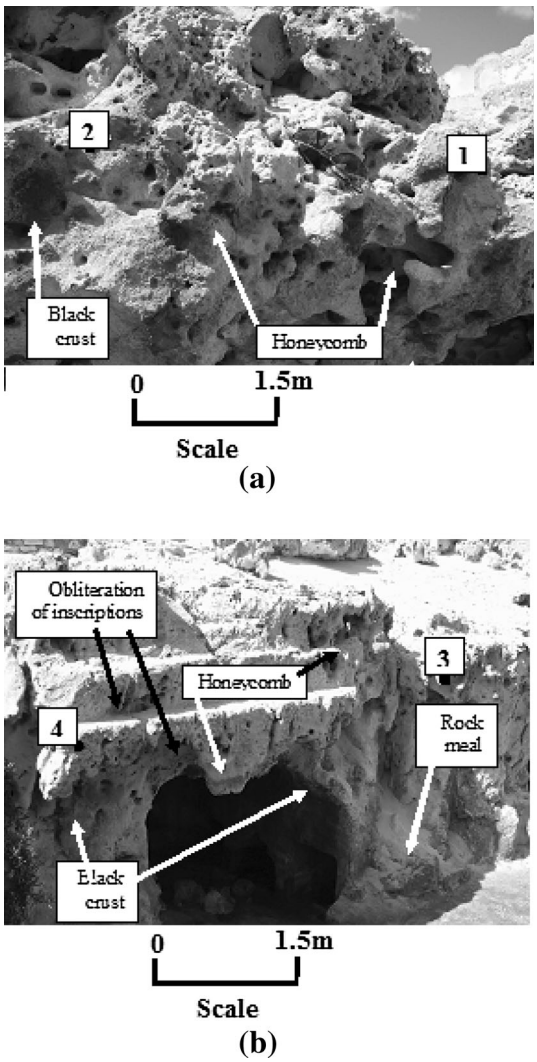

Fig. 3 El-Shatbi Tombs "east-facing wall side" with location of the collected samples. Its oolitic limestone suffers weathering forms, e.g., black crust and honeycombs (**a**), rock meal and obliteration of inscriptions (**b**)

Tombs have two major wall sides: the east- and north-facing wall sides (EFWS and NFWS, respectively). The former is normal to the seashore, whereas the latter is parallel to the sea shore (Fig. 2a, b). Such tombs present weathering forms expressed by honeycombs, rock meal, salt efflorescence, dark-colored pollutant patches at semi-sheltered parts of this site, and biological cover (Figs. 3, 4, 5). Thus, the primary aims of the current study are to determine the salt weathering impact on the oolitic limestone using the El-Shatbi Tombs as a case study and to define the damage category for the two differently oriented wall sides that are NFWS and EFWS. Additionally, this study aims to modify "for more specification" the damage category, "i.e., the grade or limit of site deterioration" scale of Fitzner and Heinrichs (2002). This is to be applicable, as a non-destructive technique, "i.e., technique that is not based on major rock sampling particularly at the sites at which sampling is not preferred due to its historical

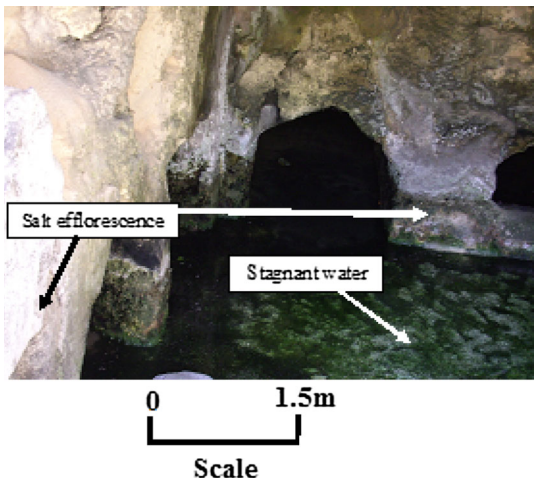

Fig. 4 El-Shatbi Tombs with salt efflorescence, domestic water flooding basal parts of El-Shatbi Tombs, east-facing wall side

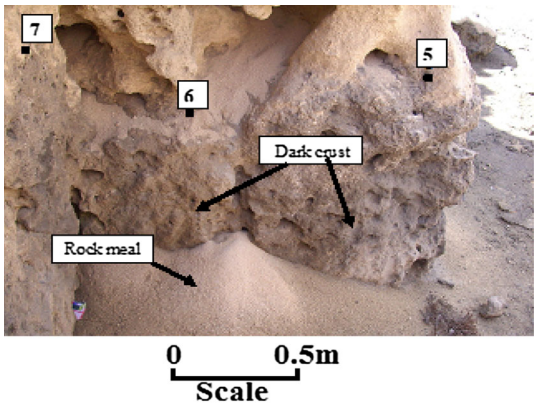

Fig. 5 El-Shatbi Tombs "north-facing wall side" with location of the collected rock samples; it presents intense rock meal, dark crust and honeycombs

importance", in this context. This information will shed light on the standards of a rock's properties most applicable for the conservation of archaeological sites in environments suffering salt-based weathering. To achieve these aims, the following field and laboratory investigations were conducted, as described in detail in the next section.

Methodology

Field and laboratory investigations were conducted to modify the damage category scale of Fitzner and Heinrichs (2002) and apply it to the El-Shatbi Tombs. Also, to investigate weathering (particularly by salts) on the rock mass of these tombs in such Mediterranean Sea climate (coastal region) using tiny rock samples from this site. The results of the laboratory investigations conducted for the weathered rock samples are compared with control rock samples, of the same rock type, collected at quarries close to Alexandria of the same bedrock and geologic age of the El-Shatbi Tombs.

Field investigations

All the weathering forms were recorded along with their dimensions (e.g., width, depth, density, thickness, length). They were then categorized into four groups following Fitzner and Heinrichs' (2002) classification:

Group 1 Loss of stone material (LS); includes back weathering represented by cavernous weathering and an equal loss of stone surface material.

Group 2 Discoloration/deposits (DD); includes loose salt deposits, e.g., salt efflorescence, pollutants as black crust and biological colonization.

Group 3 Detachment (DT); includes the separation of small or large parts of the rock body in the form of granular disintegration (rock meal), scaling and/or exfoliation.

Group 4 Fissures/deformation (FD); includes all types of fissures, i.e., single, map and multiple cracks.

Following the categorization of the weathering forms at the study area, the damage category must be defined for each area in terms of the weathering forms in each of the four groups listed above, which can be achieved using Fitzner and Heinrichs' (2002) classification as follows:

Damage category 0 No visible damage can be noted
Damage category 1 Faint damage can be noted
Damage category 2 Slight damage can be noted
Damage category 3 Moderate damage can be noted
Damage category 4 Severe damage can be noted
Damage category 5 Very severe damage can be noted

Consequently, as this classification, which is descriptive for a stone's surface weathering, is not specified in terms of limits or percentages for weathering forms, it has been modified in the current study. This is to be more specific, easily applicable and able to precisely define damage categories regarding the weathering forms mentioned in the four groups of Fitzner and Heinrichs (2002). The modified classification of the damage categories has been listed in Table 3 and graphically represented in Fig. 6. This figure (sketch) clarifies the area percentage of a given wall side, of any building or excavation, that is affected by weathering processes. This is in conjunction with back weathering (in millimeters) from a stone's surface to deep inside resulting in removal of surface inscriptions, decorations and/or paintings of a given archaeological site.

Table 3 Modification of damage category of Fitzner and Heinrichs (2002)

Damage category (DC)	Fitzner and Heinrichs (2002) DC scale	The modified DC scale in the current study
0	No visible damage	No visible damage on the stone's surface, inscriptions and/or paints
1	Faint damage	Very slight weathering on inscriptions and/or paints to less than a 1-mm depth, or less than 5 % of wall side has DD, DT and and/or LS
2	Slight damage	Slight back weathering on inscriptions and/or paints from a 1–2-mm depth, or 5–10 % of the wall side presents DD, DT, LS and/or FD
3	Moderate damage	Moderate weathering on inscriptions only, as paints are totally demolished at this DC, back weathering from a 2–5-mm depth, or 10–25 % of the wall side presents DD, DT, LS and/or FD
4	Severe damage	Severe weathering on inscriptions and main rock body as back weathering from a 5–10-mm depth, or 25–50 % of the wall side presents DD, DT, LS and/or FD
5	Very severe damage	Very severe weathering on inscriptions and main rock body as back weathering is >10 mm, or >50 % of the wall side presents DD, DT, LS and/or FD

DC damage category, *DD* discoloration/deposition, *DT* detachment, *LS* loss of stone material, *FD* fissure/deformation

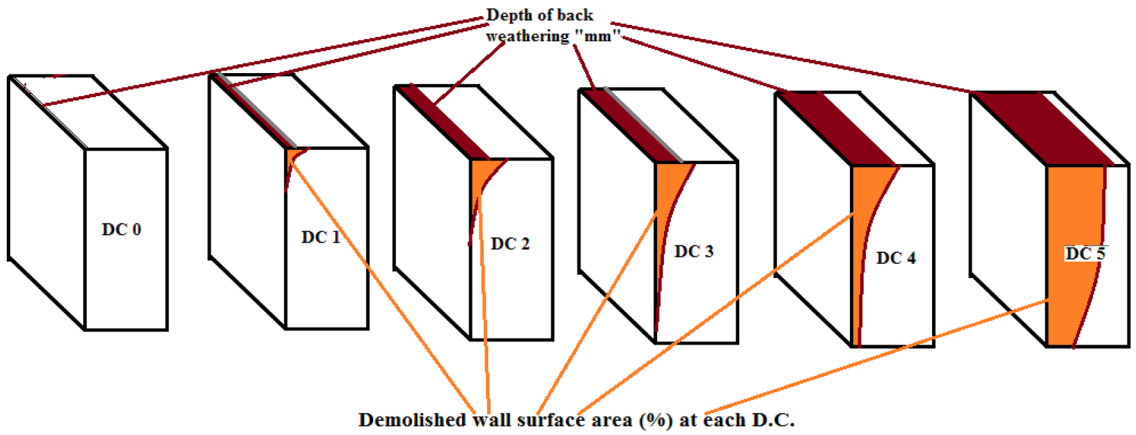

D.C. is Damage Category,
D.C. 0 = No visible damage
D.C. 1 = Faint damage (to <1mm depth or < 5% wall surface area)
D.C. 2= Slight damage (from 1-2mm depth or 5-10% wall surface area)
D.C. 3= Moderate damage (from 2-5mm depth or 10-25% wall surface area)
D.C. 4= Severe damage (from 5-10mm depth or 25-50% wall surface area)
D.C. 5= Very severe damage (to >10mm depth or >50% wall surface area)

Fig. 6 Sketch presents damage categories and their equivalent depth of back weathering and percentage of weathered wall surface area

Rock samples had also been collected at the El-Shatbi Tombs, these samples are to be used for more detailed laboratory investigations that will be explained in the following section. These samples had been collected at parts of these tombs representing weathering covering this site, e.g., samples of alveolar weathering, others of salt efflorescence and rock meal. The locations of these samples are shown on Figs. 3 and 5. The percolation of domestic water from the nearby multi-storey buildings is clearly noted from the faulty sewage pipes located at the back of these buildings, and this water accumulates at the basal parts of these tombs as shown in Fig. 4. This stagnant water has been considered in the current study as a main salt source, besides sea spray, affecting the oolitic limestone of these tombs in the prevailing climatic conditions at this coastal region.

Laboratory investigations

Laboratory investigations were conducted on seven small-sized and easily detached rock samples collected at the surface of the weathered parts of El-Shatbi Tombs (Fig. 2a) during summertime to ensure salt efflorescence from inside the tombs' rock mass to its surface. Also, small-sized

control (un-weathered) rock samples of the same rock type were collected to be taken as reference samples for the weathered samples collected at El-Shatbi Tombs. The sampling from El-Shatbi Tombs is limited for two reasons; (a) it is an archaeological site such that collecting a large number of samples or or large-sized samples is highly unrecommended or almost prohibited, (b) the recorded weathering forms covering this site are nearly the same and very characteristic for salt weathering. As such, the collected rock samples at El-Shatbi Tombs are adequate to achieve the second aim of this study. It must also be mentioned that sampling has been conducted at the stone's surface during a dry state of sampling, i.e., core sampling or sampling with a cutting machine using water was not done due to the reasons mentioned in point (a) of this section. Three stagnant water samples were also collected to be hydrochemically analyzed to find out their total dissolved salts (TDS) and salt types. This will be correlated with the hydrochemical analysis of the extracted solutions of the weathered rock samples to find out if this stagnant water is a salt source for the rock constituting these tombs or not. The laboratory investigations were conducted using the following techniques to achieve the aims of the current study.

Microscopic and mineralogical study

The rocks under investigation, either the weathered rock or the control of the same rock type, have been checked and identified based on their fabric and mineralogy (as these parameters control a rock's weathering susceptibility as well as its geotechnical property limits). So, microscopic studies have been conducted for the weathered rock samples collected at the NFWS and EFWS as well as for two control samples through thin-section investigation using a transmitting polarizing microscope (BA300T-POL, China). For more details on the rock's weathering at the micro-scale, a scanning electron microscopic study (Shmadzu, S-2400) has also been conducted for four (out of the seven) weathered rock samples collected at the two walls under investigation. These four samples had been selected based on their representation for all weathered parts at these tombs, from the visual distinction point of view, and after microscopic (thin-section) investigations for the whole collected rock samples. X-ray diffraction (using a Hitachi DS-300) analysis, as the only technique that can be used to detect all of a rock's mineralogy, has also been used to detect all the rock's possible mineral and salt content ($2\theta = 4$–$70°$, 40 kV, 2°/s). It has been applied for the weathered and control samples of this rock type. The auto-identified X-ray diffractograms of these samples are presented in the results section of this study.

Rock and pore properties

As salt weathering, with its diagnostic features, can easily be noted on the limestone of these tombs, the rock's susceptibility to salt attack were considered for the area under investigation. This was achieved by measuring the pore properties of two small rock samples collected at the NFWS and EFWS as well as three control samples, using mercury intrusion porosimetry (MIP-5900, Hitachi Comp., Japan) at low and high mercury pressures (31.00 and 33000 psi, respectively) to access all rock micro- and nano-pores. Using MIP, the following parameters were measured: mean pore diameter, bulk and skeletal densities, porosity and pore size distribution (PSD). The salt susceptibility index (SSI) of these facies has been computed using Yu and Oguchi's (2010) equation:

$$\mathrm{SSI} = \left(I_{\mathrm{pc}} + I_{\mathrm{pm}\,0.1}\right)\left(P_{\mathrm{m5}}/P\mathrm{c}\right)$$

where I_{pc} is the index of connected pores; $I_{\mathrm{pm}\ 0.1}$ is the index of 0.1-μm-radius micro-pores; P_{m5} is the volume of the 5-μm-radius rock micro-pores, and Pc is the volume of the connected pores.

The classes of SSI, I_{pc}, and $I_{\mathrm{pm0.1}}$ have been given by Yu and Oguchi (2010). The SSI of a given rock can be categorized using Yu and Oguchi's (2010) classification, from exceptionally salt-resistant to exceptionally salt-prone (Table 4). This classification was modified in the current study to better clarify and numerically specify the SSI category by adding the category scale (0–5) and adding salt resistance terminologies that are widely used in the field to assess a rock's durability to salts (Table 4).

Using the SSI classification (Table 4), the SSI class of the examined rock samples can then be defined; also, the damage category of the rock under investigation can be correlated with its SSI.

Hydrochemical analysis

Salt weathering diagnostic features on the surface of these tombs were recorded. The total dissolved salts (TDS) and salt type and percentage have been determined using

Table 4 Salt susceptibility index (SSI) and its ranking (Yu and Oguchi 2010)

SSI	Interpretation	Ranking
$0 \leq \mathrm{SSI} < 1$	Exceptionally salt-resistant	0
$1 \leq \mathrm{SSI} < 3$	Very salt-resistant	1
$3 \leq \mathrm{SSI} < 7$	Salt-resistant	2
$7 \leq \mathrm{SSI} < 10$	Salt-prone	3
$10 \leq \mathrm{SSI} < 15$	Very salt-prone	4
$15 \leq \mathrm{SSI} < 20$	Exceptionally salt-prone	5

titration and a flame photometer. This analysis has been conducted for the extracted salt solutions prepared from the collected, weathered and control rock samples using Rhoades's (1982) method (1:5 ratio of soil:distilled water). The hydrochemical analysis has also been conducted for the stagnant water samples collected at the study area. This is to provide a comprehensive explanation of the salt weathering at the El-Shatbi Tombs.

Hydrochemical analysis was conducted for seven rock samples collected at the weathered parts of the site, four control samples of the same rock, and three stagnant water samples at these tombs. Sampling was conducted in the summertime to ensure that the salts within the weathered limestone were withdrawn close to or at the stone's surface in such semi-arid conditions.

Rock geotechnical properties

Besides the rock and pore properties that indicate the PSD that controls a rock's SSI, the geotechnical properties (measured by the magneto-structive ultrasonic waves) throw light on the weathering grade of a given rock. Simply, the velocity of these waves (*C*p) measured for a given rock is decreased on increasing the rock's weathering grade on one hand, while the rock's internal friction (*Q*c) is increased on increasing the rock's weathering grade on the other hand (Kapranos et al. 1981; Calleja et al. 2000). Consequently, these properties were measured for the rock samples collected at the EFWS and NFWS using magneto-structive ultrasonic wave equipment (Fig. 7; MSU-3000, Ukraine) following the method of Kapranos et al. (1981). Additionally, the corresponding properties of the control rock samples were measured to numerically determine the damage category of the weathered limestone based on the recession of the limits of their geotechnical properties. The measured geotechnical parameters are the velocity of the ultrasonic waves (*C*p), the rock's internal friction (*Q*c), and the rock's elastic modulus (Ed). Equations from Kapranos et al. (1981), listed below, were used to compute *C*p, *Q*c, and Ed:

$$[(A_o + A_t)/(A_o - A_t)] = X$$

$$Qc = \{\pi n (1 + X)\}/\{\ln[2/(1 - X)]\}$$

$$Cp = 2\,Lf/n$$

$$Ed = \rho\, Cp^2$$

where A_o and A_t are the initial and steady magnitude of the ultrasonic waves, respectively; n is the mode number at which we obtain the best echo form for the waves (Fig. 7); *Q*c is the material's internal friction; *C*p is the velocity of the ultrasonic waves (km/sec); L is the sample's length (cm); f is the frequency of the waves (kHz); Ed is the elastic modulus of the material under investigation (GPa); and ρ is the density of the material (g/cm^3).

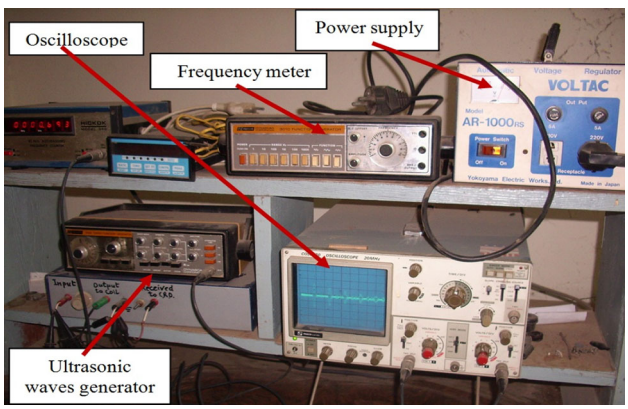

Fig. 7 Magneto-structive ultrasonic equipment with best echo-form on its screen

Results

Field data and data processing

The El-Shatbi Tombs were considered in the current work as they experience variable limits and forms of weathering, as those recorded on most of Greco-Roman sites on the Mediterranean Sea coast of Egypt, affecting their historical value. The study area is located close to the Mediterranean Sea, around 50 m distant from the shoreline. The location and geometry of El-Shatbi Tombs can be noted in Fig. 2a and b.

The weathering forms and their dimensions at El-Shatbi Tombs are listed in Table 5 to define the rock's damage category at the two wall sides composing these tombs using the DCAW scheme of Fitzner and Heinrichs (2002; Fig. 8). Some of the recorded weathering forms indicated very severe damage at each of the seven checkpoints (Table 5), e.g., the obliteration of inscriptions. Others experienced severe damage, e.g., salt efflorescence and granular disintegration; moderate damage, e.g., black crust and scaling; or very slight damage, e.g., fissures (Table 5). Then, the average value of damage category regarding each weathering form at the check points of each wall side has been defined (Table 5). This is to get the overall damage category for the NFWS and EFWS considering all weathering forms together using the DCAW scheme. This overall DC for each wall side has been achieved by the intersection of the average DC for the four weathering groups DCLS, DCDD, DCDT and DCFD on the DCAW scheme. The new achievement is that the two wall sides of these tombs have a very severe damage category (Fig. 8). The colors presented in the DCAW indicate the damage category defined

Table 5 Weathering forms and their dimensions; average and the overall damage categories based on the refined scale and the DCAW scheme of [1]; El-Shatbi Tombs, Alexandria City

Site of investigation	Wall side orientation and points of concern	Weathering forms and its dimensions								
		Group I loss of stone material (LS)			Group II discoloration/deposits (DD)					
		Back weathering (W)		Damage category	Loose salt deposits (E)		Damage category	Pollutants (P)		Damage category
		Obliteration of inscriptions (OI)			Salt efflorescence (SE)			Black crust (BC)		
		Area (%)	Depth (mm)		Area (%)	Thickness (mm)		Area (%)	Thickness (mm)	
El-Shatbi Tombs	East-facing wall side [EFWS]									
	1	100	30	5	37	3	4	17	2	2
	2	99	35	5	25	4	4	12	2	2
	3	100	34	5	38	3	4	18	2	2
	4	100	33	5	40	2.5	4	15	1	2
	Average damage category for EFWS based on the refined scale of Fitzner and Heinrichs (2002)	5 Very severe damage category			4 Severe damage category			3 Moderate damage category		
	Overall DC for EFWS based on DCAW of Fitzner and Heinrichs (2002)	5 Very severe damage category regarding all weathering forms								
	North-facing wall side [NFWS]									
	5	100	27	5	45	5	4	11	1	3
	6	100	25	5	50	6	4	8	1	3
	7	98	28	5	48	5.5	4	12	0.5	3
	Average damage category for NFWS based on refined scale of Fitzner and Heinrichs (2002)	5 Very severe damage category			4 Severe damage category			2 Slight damage category		
	Overall DC for NFWS based on DCAW of Fitzner and Heinrichs (2002)	5 Very severe damage category regarding all weathering forms								

Table 5 continued

Site of investigation	Wall side orientation and points of concern	Weathering forms and its dimensions									
		Group III detachment (DT)						Group IV fissures/deformation (FD)			
		Granular disintegration (RM)		Damage category	Scaling (S)		Damage category	Fissures (L)			Damage category
		Area (%)	Depth (mm)		Area (%)	Thickness (mm)		v.L.			
								Width (mm)	Length (m)	Density/m2	
El-Shatbi Tombs	East-facing wall side [EFWS]										
	1	50	30	4	12	3	3	2	0.5	0.5	2
	2	46	35	4	9	5	2	0	0	0	0
	3	40	34	4	11	4	3	0	0	0	0
	4	40	33	4	10	4	3	4	0.3	1	2
	Average damage category for EFWS based on the refined scale of Fitzner and Heinrichs (2002)	4 Severe damage category			3 Moderate damage category			1 Faint damage category			
	Overall DC for EFWS based on DCAW of Fitzner and Heinrichs (2002)	5 Very severe damage category regarding all weathering forms									
	North-facing wall side [NFWS]										
	5	35	27	4	15	4	3	3	0.2	1	2
	6	29	25	4	14	5	3	3	0.3	1	2
	7	31	28	4	15	5	3	0	0	0	0
	Average damage category for NFWS based on refined scale of Fitzner and Heinrichs (2002)	4 Severe damage category			3 Moderate damage category			1 Faint damage category			
	Overall DC for NFWS based on DCAW of Fitzner and Heinrichs (2002)	5 Very severe damage category regarding all weathering forms									

by the modified DC scale (Table 3) for each of the four groups of weathering forms, the dotted number "5" inside this scheme is the overall DC of each wall side.

Laboratory investigations

The laboratory investigations included microscopic, mineralogical, rock and pore properties; limits of the rock's geotechnical properties and the rock's salt content have been investigated for the weathered rock samples collected at the study area as well as for the control rock samples to achieve the aims of the current study.

Mineralogical and microscopic investigations

The mineralogical investigation was conducted in the current study using X-ray diffraction for three rock samples collected at the weathered parts of the NFSW and EFSW and two control samples of the same rock type at oolitic limestone quarries close to the study area. The results indicated that calcite is the main mineral composing this rock (Fig. 9a–d); thus, it can be classified as a high-purity carbonate rock (Harrison et al. 1994). Silica, e.g., quartz, that was detected in a very low counts on X-ray diffractograms (Fig. 9a, b) is almost a secondary mineral representing the nuclei of such ooids. Salts were also detected, particularly halite (Fig. 9a, c).

Fig. 9 X-ray diffracto-graph presenting the mineralogical composition of the weathered limestone samples "no. 7" at the NFWS (**a**), EFWS (**b**) and (**c**) "samples no. 2 and 3" of El-Shatbi Tombs; and control samples (**d**) ▶

The fabric of the weathered and control samples was investigated through thin sections using a transmitting polarizing microscope. The rock under investigation is oolitic limestone of a packstone to wackestone nature (oosparite to oo-micro-spar, Fig. 10) based on Dunham classification (1962). Halite and gypsum have been identified based on their optical properties only for the examined thin sections of the weathered samples of El-Shatbi Tombs (Fig. 10a).

The detection of weathering features on the micro-scale for the site under investigation was conducted using scanning electron microscopy for the collected weathered samples. The results indicated that the rock under consideration is suffering micro-pitting and onion exfoliation (McGreevy 1985 and Dearman 1995 terminologies) of the ooids' lamella (Fig. 11a, b). The EFWS samples displayed a relatively higher rank of micro-scale deterioration than the NFWS, e.g., fragmentation and loosening of the microstructure of the ooids and their surrounding micro-spars

Fig. 8 DCAW scheme indicating the overall damage category of the north- and east-facing wall sides at El-Shatbi Tombs considering all weathering forms

DCLS		DCDD 0				1			2			3				DCDT
		4	4	5	4	4	5	4	4	5	4	4	5	4	
		3	3	4	3	3	4	3	3	4	3	3	4	3	
	0	2	2	3	2	2	3	2	2	3	3	3	3	2	
		1	2	3	2	2	3	2	2	3	3	3	3	1	
		0	2	3	2	2	3	2	2	3	3	3	3	0	
		4	4	5	4	4	5	4	4	5	4	4	5	4	
		3	3	4	3	3	4	3	3	4	3	3	4	3	
	1	2	2	3	2	2	3	2	2	3	3	3	3	2	
		1	2	3	2	2	3	2	2	3	3	3	3	1	
		1	2	3	2	2	3	2	2	3	3	3	3	0	
		4	4	5	4	4	5	4	4	5	4	4	5	4	
		3	3	4	3	3	4	3	3	4	3	3	4	3	
	2	2	3	3	3	3	3	2	3	3	3	3	3	2	
		2	2	3	2	2	3	2	2	3	3	3	3	1	
		2	2	3	2	2	3	2	2	3	3	3	3	0	
		5	5	5	5	5	5	5	5	5	5	5	5	4	
		4	4	5	4	4	5	4	4	5	4	4	5	3	
	3	3	3	4	3	3	4	3	3	4	3	3	4	2	
		3	3	4	3	3	4	3	3	4	3	3	4	1	
		3	3	4	3	3	4	3	3	4	3	3	4	0	
		5	5	5	5	5	5	5	5	5	5	5	5	4	
		5	5	5	5	5	5	5	5	5	5	5	5	3	
	4	4	4	5	4	4	4	4	4	5	4	4	5	2	
		4	4	5	4	4	5	4	4	5	4	4	5	1	
		4	4	5	4	4	5	4	4	5	4	4	5	0	
		5	5	5	5	5	5	5	5	5	5	5	5	4	
		5	5	5	5	5	5	5	5	5	5	5	5	3	
	5	5	5	5	5	5	5	5	5	5	5	5	5	2	
		5	5	5	5	5	5	5	5	5	5	5	5	1	
		5	5	5	5	5	5	5	5	5	5	5	5	0	
		0	2	3	0	2	3	0	2	3	0	2	3		
		DCFD													

N.B. DCLS is Group 1 of weathering forms "Loss of Stone Material"; DCDD is Group 2 of weathering forms "Discoloration/Deposits"; DCDT is Group 3 of weathering forms "Detachment"; and DCFD is Group 4 of weathering forms "Fissures/Deformation".

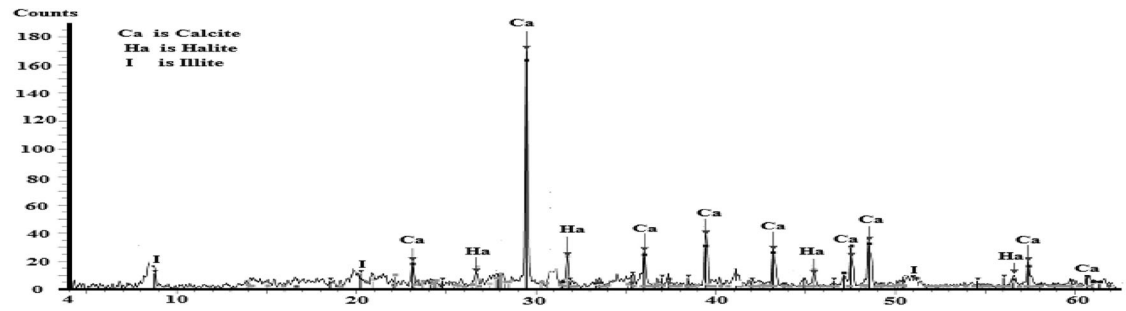
Counts
Ca is Calcite
Ha is Halite
I is Illite

(a)

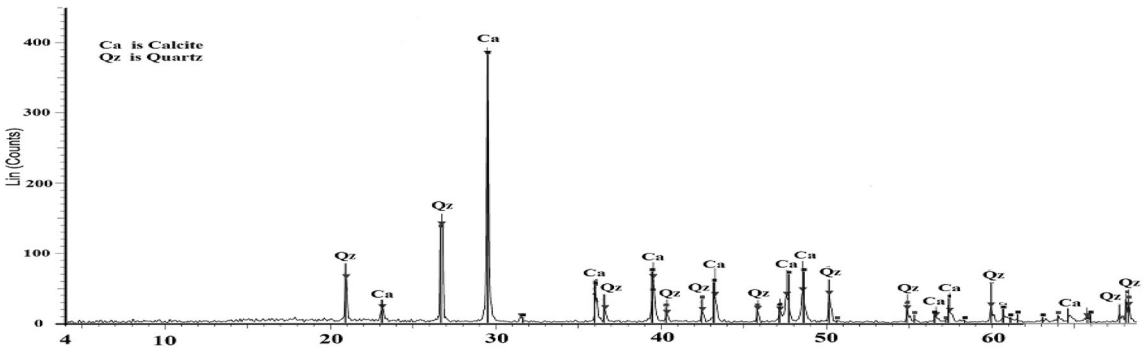
Ca is Calcite
Qz is Quartz
Lin (Counts)

(b)

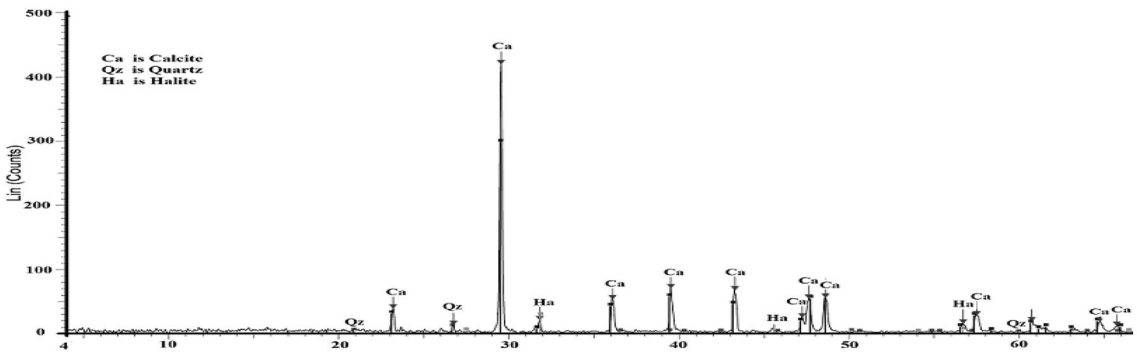
Ca is Calcite
Qz is Quartz
Ha is Halite
Lin (Counts)

(c)

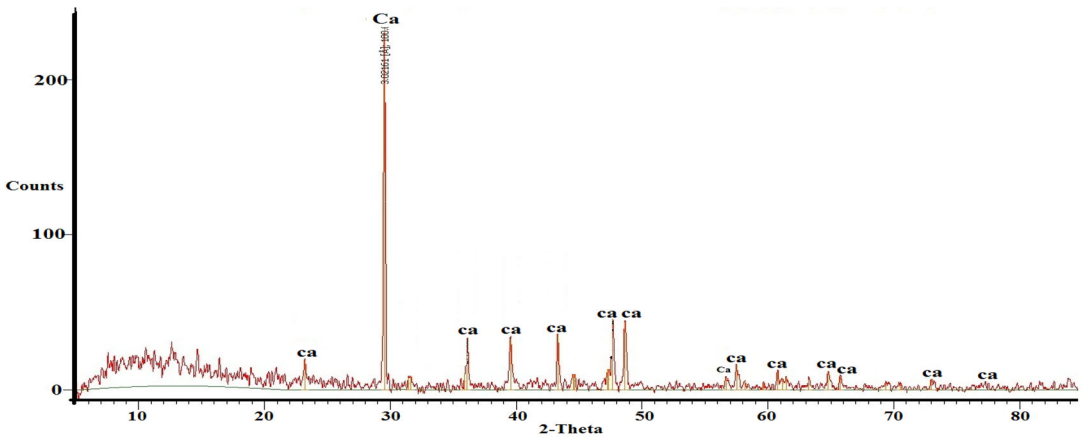
Counts
2-Theta

(d)

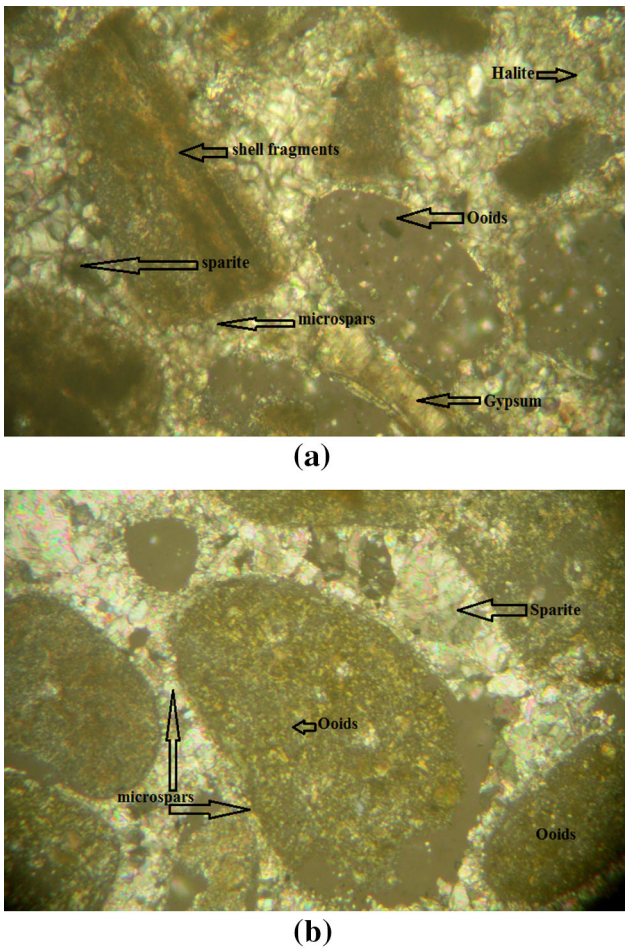

Fig. 10 Representative thin section presenting the packstone to wackestone fabric of the weathered oolitic limestone of El-Shatbi Tombs (crossed nicoles, 40×) (**a**); and packstone to wackestone of the control oolitic limestone (crossed nicoles, 40×) (**b**)

(Fig. 11a, b). With the aid of electron dispersive X-ray (EDX), as an assistant unit inserted in the scanning electron microscope, halite and gypsum were identified in the SEM field of view coating the rock's components and filling its pores for most of the examined samples (Fig. 11c), while the control samples of the same rock type had fabric free from salts and weathering features at the micro-scale (Fig. 11d).

Rock and pore properties

Determining the rock and pore properties is of value in defining a rock's susceptibility to weathering, particularly by salts (SSI), and to identify the main contributor(s) to the rock's DC, e.g., PSD. Mercury intrusion porosimetry has been used for three control samples and two weathered samples from the NFWS and EFWS (Table 6). After data processing and using the SSI classification of Yu and Oguchi (2010; Table 4), it was determined that the control rock is salt-resistant (rank 2, Table 6), whereas the weathered rock at El-Shatbi Tombs is classified within the deleterious SSI categories, i.e., very salt-prone (rank 4) and exceptionally salt-prone (rank 5) for NFWS and EFWS, respectively (Table 6). Additionally, the PSD is distinctly different for the control and weathered samples at the two wall sides of El-Shatbi (Table 6). This PSD (%) will be correlated with SSI and DCAW to determine its participation in the susceptibility of the rock to weathering, especially by salts.

Hydrochemical analysis results

It can be noted that the weathered parts of these tombs have TDS values ranging from 13985 to 16478 ppm for the NFWS and 22811 to 27546 ppm for the EFWS (Table 7), approximately 1.5 times that of the NFWS. Chlorides, particularly halite, are the most prevalent, followed by sulphates (particularly $CaSO_4$ salt) for the examined rock samples. The stagnant water flooding this site, particularly at the EFWS, has TDS values ranging from 4011 to 4317 ppm, with chloride salts dominating over sulphates (Table 7). The control samples have TDS values ranging from 198 to 263 ppm; thus, the NFWS and EFWS weathered limestone have TDS values that are 65 and 109 times those of the control samples, respectively. The main reason(s) behind this high TDS at both sides of these tombs as well as the much higher TDS in the EFWS than NFWS and the inter-relation between the rock's TDS (Table 7) and the SSI (Table 6) all will be clarified and discussed in the discussion section of this current work.

Geotechnical properties results

The ultrasonic waves generated from a magneto-structive ultrasonic wave tool have been previously reported to be used to numerically determine the limit of the geotechnical properties of a given rock (Allison 1988; Calleja et al. 2000). Consequently, this equipment (Fig. 7) has been used in the current study for the weathered rock samples compared with the corresponding control samples. Seven rock samples (four from the EFWS and three from the NFWS) at this site and four control samples were tested; the results are listed in Table 8. The average values of *C*p and Ed are higher for EFWS than for NFWS, whereas the reverse is true for *Q*c. The rock under investigation is characterized by lamination numerically recognized by the difference in the velocity of the ultrasonic waves measured in two directions, parallel to and at right angle to the lamination, where *C*p is faster in the former direction than the latter. This difference, in *C*p, is directly proportional to the rock's weathering grade; the micro-gap at the lamination surface is greater for rocks that have experienced more advanced

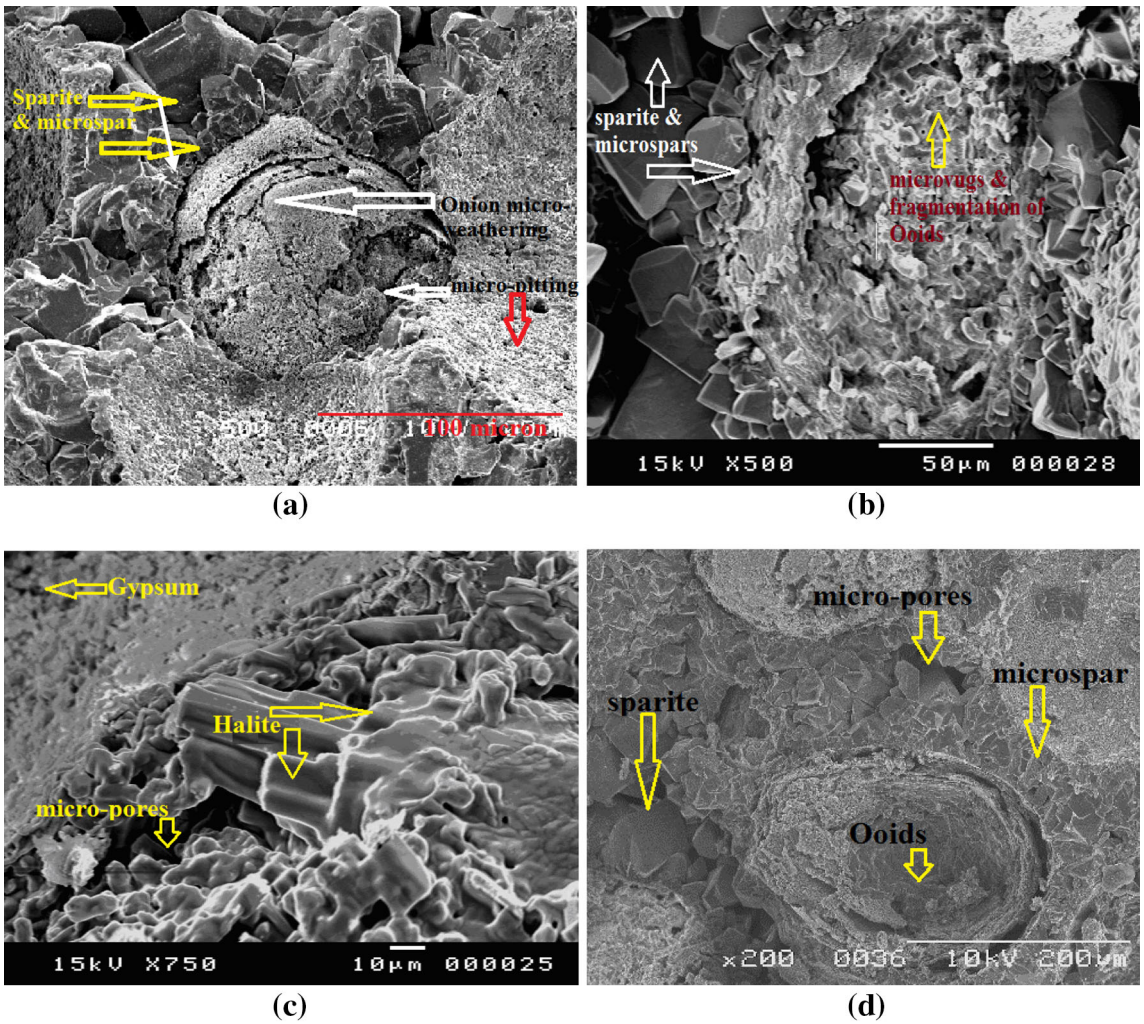

Fig. 11 Scanning electron photo-micrograph presenting an oolitic fabric with sparite and microspar crystals as the rock's matrix, onion micro-weathering and micro-pitting on oolites, EFWS (**a**); weathering features at a micro-scale in the ooid and its surrounding sparite matrix, NFWS (**b**); halite and gypsum in a crystalline form coating the rock's components, NFWS and EFWS (**c**) of El-Shatbi Tombs; and rock fabric and composition of the control sample of this rock type (**d**)

weathering, which reduces the velocity of the ultrasonic waves (Table 8).

Discussion

Defining the damage category of a given rock, particularly those at archaeological sites, is of value for gauging the necessity for restoration or correlating the rate of weathering of different units at a given area or at two separate areas of investigation. Also, it enables specification of the rock's parameters that control its weathering susceptibility to be avoided when choosing rock for further building or restoration. The damage category was determined before using the scale of Fitzner and Heinrichs (2002) that might be unspecified even for the same researcher. Consequently, this classification has been modified in the current study by specification of the limits of the weathering forms in the four groups of weathering form (DCLS, DCDD, DCDT, DCFD; Table 3). The DCLS is group no. 1 that means a damage category resulting in loss of stone material by some related weathering forms; while DCDD is group no. 2 that means a damage category resulting in discoloration/deposits altering the stone's surface color; DCDT is group no. 3 that means a damage category resulting in detachment of a stone's material by some related weathering forms; and DCFD is group 4 that means a damage category resulting in fissures/deformation for a given building by some related weathering forms listed for the four groups of weathering forms in Fitzner and Heinrichs (2002).

This classification has been applied for Greco-Roman tombs on the Mediterranean Sea of Egypt. It has been indicated that DCLS (mainly as obliteration of inscriptions) and DCDT (mainly as granular disintegration and scaling)

Table 6 Measured and computed rock and pore properties, based on Yu and Oguchi 2010 and their refined classification, for control and weathered parts at El-Shatbi Greco-Roman Tombs

Sample's location	Geographic orientation	Sample's description	Sample code	Rock and pore properties							
				Incremental pore volume (IPV)	Volume of pores <0.1 μm (mL/g)	Volume of pores <5 μm (mL/g)	Total connected porosity (*Pc* %)	Average Microporosity <0.1 μm "*P*m0.1 %" regarding Pc	Average Microporosity <5 μm "*P*m5 %" regarding Pc	*I*pc	*I*pm0.1
Control bedrock	Deep Seated samples at Pliestocene Ridges	Control (Un-weathered) samples	C 1	0.088	0.0021	0.083	22.1	0.14	19.89	6	1
			C 2	0.086	0.0019	0.079	22.4				
			C 3	0.088	0.002	0.081	22.2				
El-Shatbi Tombs (Weathered bedrock)	North Facing Wall Side "NFWS"	Weathered	1-NFWS	0.1884	0.1001	0.18	25.47	13.66	24.05	7	7
			2-NFWS	0.1999	0.1116	0.193	24.65				
	East Facing Wall Side "EFWS"	Weathered	3-EFWS	0.228	0.14	0.22	31.47	20.12	31.28	8	10
			4-EFWS	0.238	0.15	0.231	33.26				

Sample's location	Geographic orientation	Sample's description	Sample code	Rock and pore properties						
				*P*m5/*P*c	SSI value	SSI interpretation	Pore size distribution (PSD % VTP)			
							<0.01 μm	0.01–0.1 μm	0.1–1.0 μm	1.0–10 μm	10–100 μm
Control bedrock	Deep Seated samples at Pliestocene Ridges	Control (Un-weathered) samples	C 1	0.91	6.38	Salt resistant (2)	0.00	1.01	19.89	77.57	3.53
			C 2				0.00	1.04	20.37	79.44	3.62
			C 3				0.00	1.07	19.89	77.57	3.53
El-Shatbi Tombs (Weathered bedrock)	North Facing Wall Side "NFWS"	Weathered	1-NFWS	0.96	13.44	Very salt prone (4)	18.40	43.40	7.52	29.32	1.34
			2-NFWS				21.90	41.60	7.20	28.10	1.28
	East Facing Wall Side "EFWS"	Weathered	3-EFWS	0.97	17.4	Exceptionally salt prone (5)	0.77	62.80	9.10	25.70	1.62
			4-EFWS				2.58	65.70	8.60	21.60	1.53

Ipc index of connected pores, *Ipm0.1* index of 0.1-μm-radius micro-pores, *Pm5* volume of the 5-μm-radius rock micro-pores, *Pc* volume of the connected pores, *SSI* salt susceptibility index, *PSD* is pore size distribution, *VTP* total pore volume

Table 7 Hydrochemical analysis for weathered and control oolitic limestone and the stagnant water flooding El-Shatbi Tombs

Site of study	Part of investigation	Sample code	TDS (ppm)	EC (mmohs/cm)	Cations (ppm)				Anions (ppm)			
					Ca++	Mg++	Na+	K+	Cl−	SO4−	CO3−	HCO3−
El-Shatbi Tombs	East-facing wall side (EFWS)	1	27546	12.8	5576	1117	6112	1321	4984	6870	567	999
		2	22811	10.7	5170	989	5764	768	5110	4707	0	303
		3	25907	11.3	4923	1210	5589	987	5229	6234	476	1259
		4	26188	12.1	4989	1762	6223	1034	5314	6102	211	553
	North-facing wall side (NFWS)	5	15498	7.2	2564	634	3988	176	4120	3156	126	734
		6	16478	7.8	3657	733	4100	367	3875	2784	243	719
		7	13985	6.9	2687	1124	3879	738	3652	1874	0	31
	Stagnant water	Stag-1	4317	4.9	1587	84	786	46	984	765	12	53
		Stag-2	4011	4.8	1213	70	699	65	875	983	37	69
		Stag-3	4100	4.8	1324	59	867	22	945	769	23	91
Quarried samples	Control samples	Con-1	234	2.1	87	12	48	0	42	32	0	13
		Con-2	263	2.3	76	9	39	11	51	49	0	28
		Con-3	244	2.1	54	23	46	15	50	52	0	4
		Con-4	198	2	37	13	41	8	46	28	0	25

Site of study	Part of investigation	Sample code	Hypothetical dissolved salts (%)								
			KCl	NaCl	$CaCl_2$	Na_2SO_4	$CaSO_4$	$MgSO_4$	$MgCO_3$	$CaHCO_3$	$Mg(HCO_3)_2$
El-Shatbi Tombs	East-facing wall side (EFWS)	1	5.1	38.9	0	0.2	41.9	2.9	5.9	0	5.1
		2	3.3	40.5	14.2	0	28.5	11.5	0	0	2
		3	4.1	39	5.9	0	34.4	9.6	0	0	6.9
		4	3.9	38.5	8.6	0	27.7	15.3	2.4	0	3.4
	North-facing wall side (NFWS)	5	1.3	47.8	9.9	0	26.2	6.8	2.1	0	6
		6	2.2	40.8	15	0	27.7	3.3	4.3	0	6.3
		7	4.6	40.1	27.3	0	5.3	21.7	0	0	0.4
	Stagnant water	Stag-1	1	27.6	33.4	0	32.2	2.8	0.9	0	1.9
		Stag-2	1.7	30.4	19.9	0	42.1	0.9	2.6	0	2.4
		Stag-3	0.5	34	24.5	0	36	0	1.2	0	3.3
Quarried samples	Control samples	Con-1	0	27.6	29.4	0	29.4	2.6	0	0	10.3
		Con-2	4.3	25.6	19.1	0	35	0	0	4.4	11.3
		Con-3	5.5	28.1	21.4	0	17.4	24.6	0	0	2.6
		Con-4	4.2	35.7	17.1	0	20.8	4.2	0	0	17.9

EC electrical conductivity of the samples' extracted solutions, *TDS* total dissolved salts of the extracted solution, *Stag.* stagnant water sample at these tombs, *Con.* control rock sample

are the main controlling weathering groups for the DCAW at the NFWS and EFWS (Table 5).

For investigating the factors causing and controlling weathering at the study area, laboratory investigations were conducted to semi-quantify the outcome of this weathering. The petrographic and mineralogical investigations for the weathered samples and the equivalent control samples revealed that the samples are of oolitic limestone of high purity as they contain high percentages of carbonates (mainly calcite, Figs. 9, 10, 11). This high-purity carbonate rock is a good material for weathering processes to act on it with high rates of weathering (Harrison et al. 1994). The rock's salt content, almost halite and gypsum, was detected in the thin sections and SEM fields of investigation only for the weathered samples (Figs. 10a, 11c). These visually defined salts with their associated weathering forms at a micro-scale (micro-pitting, micro-fragmentation, onion micro-weathering, Figs. 10a and 11a–c) have been numerically proved through the hydrochemical analysis conducted for the weathered and control samples (Table 7). This analysis proved that halite and gypsum are the main salts invading the rock's pores of this site, exerting high stresses on rock pores leading to such weathering at a macro-scale (Figs. 3, 5) and micro-scale (Fig. 11a–c; Kay et al. 1981; Flatt 2002). The source of these salts at both sides of these tombs is expected to be a mixture of two

Table 8 Ultrasonic waves parameters measured for the weathered and control limestone at El-Shatbi Tombs

Site of study	Wall of investigation	Sample code	Ultrasonic parameters					
			Cp 1 (km/sec) parallel to lamination	Cp 2 (km/sec) at right angle to lamination	Average Cp (km/sec)	Iso-tropism (Cp1/Cp2)	*Qc*	Ed
El-Shatbi Tombs	East-facing wall side	1	1.88	1.68	1.78	1.12	9.5	6.97
		2	1.85	1.65	1.75	1.12	9.8	6.74
		3	1.87	1.71	1.79	1.09	9.1	7.05
		4	1.86	1.66	1.76	1.12	9.3	6.81
	Average value for four weathered samples atthe east-facing wall side		1.87	1.68	1.77	1.11	9.43	6.89
	North-facing wall side	5	1.76	1.51	1.64	1.17	9.9	5.88
		6	1.71	1.42	1.57	1.20	10.5	5.39
		7	1.73	1.43	1.58	1.21	10.3	5.49
	Average value for three weathered samples at the north-facing wall side		1.73	1.45	1.59	1.19	10.23	5.59
	Quarried samples *control or Rrference samples*	Con-1	2.01	1.94	1.98	1.04	7.9	8.58
		Con-2	2.11	1.99	2.05	1.06	7.4	9.25
		Con-3	2.12	1.97	2.05	1.08	7.4	9.20
		Con-4	2.06	1.95	2.01	1.06	7.1	8.84
	Average value for Con 1–4		2.08	1.96	2.02	1.06	7.45	8.97

Cp1 velocity of the ultrasonic waves measured parallel to the rock's lamination, *Cp2* measured at a right angle to Cp1 for the same sample, *Qc* rock's internal friction, *Ed* rock's elastic modulus

sources, sea water and human domestic water, at different ratios (Kamh 2000). Sea water reaches these tombs as sea spray and sub-surface percolation where these tombs are very close to sea shore (Kamh 2000). Human domestic water reaching these tombs is highly expected as these tombs lie at the foot level of these recent buildings with their leaking pipes (Fig. 2b). In general, the type of salt content of stagnant water and the weathered rock of these tombs is highly matched (Table 7). Air pollutants have been recorded, in previous literature, being captured on rough, wet and un-even surfaces (McGreevy 1996). These air pollutants are adsorbed on the rough, wet surface of this oolitic limestone and deeply sink in the surficial pores of this porous rocks (which have total connected porosities ranging from 25 to 32%, for the NFWS and EFWS, respectively, Table 6). These pollutants, which are not well-recorded by a specified institution at the study area, are either chemically reactive with this pure carbonate rock, forming salts of a chemical origin (chlorides and sulfates of calcium), or deposited on the semi-sheltered stone's surface altering its white color into dark grey (Fig. 5). These salts (particularly the hygroscopic ones, chlorides) pass through weak planes and micro-planes (intra-lamina micro-planes), exfoliating them into an onion-like micro-fabric (Fig. 11a), or disintegrate these ooids and the rock's matrix (micro-spars and sparite, Fig. 11b). Rock's textural deformation by salts' ingress creates an onion-like micro-fabric and fragments the rock's components (Figs. 3, 4, 5), firstly resulting in increasing the rock's micro-porosity and total connected porosity (Hall and Hoff 2007; Steiger and Asmussen 2008; Yu and Oguchi 2010; Hall et al. 2010), e.g., from 19.84 and 22%, respectively, (for the control limestone) to 24 and 25% for the weathered NFWS and to 31.3 and 32% for the EFWS, respectively (Table 6). The weathering by these salts has also been recorded on a macro-scale (on EFWS and NFWS) by the diagnostic features presented in Figs. 3, 4 and 5 and listed with their dimensions in Table 5. After that, salt accumulation and crystallization (at climatic conditions prevailing in the Middle East), besides micro-fragmentation of the rock's components (allochems and matrix, Fig. 11a, b), reduced the dimensions (mainly the radii) of the rock's pores, altering the mega-pores to micro-pores (Hall and Hoff 2007; Steiger and Asmussen 2008; Hall et al. 2010); i.e., the rock's PSD has been altered (on micro-fragmentation of the rock's components and/or salt accumulation within these pores) from the pores with radii almost ranging from 1 to 10 microns (representing 78% of the Pc for the control rock), to the range 0.01–0.1 microns (representing 42% of Pc for NFWS and 64% of the *Pc* for the EFWS, Table 6). It has been previously reported that not all ranges or limits of micro-pores increase a rock's susceptibility to salt weathering (Steiger and Asmussen 2008; Yu and Oguchi 2010); i.e., the pore radius distribution may increase or decrease the rock's susceptibility to salt weathering (Yamashita and Suzuki 1986). In the

current study, the alteration of rock pore size resulted in increasing a rock's susceptibility to weathering where its salt susceptibility class has been altered from salt-resistant with SSI = 6.38 (for the control samples) to very salt-prone with SSI = 13.44 (for NFWS) and to exceptionally salt-prone with SSI = 17.4 (for EFWS; Table 6).

The orientation of a given wall side controls the number and intensity of weathering cycles acting on it (Kay et al. 1981; Mustoe 1983; Thomachot et al. 2011). In the current study, the EFWS is expected to receive relatively more salt weathering and/or wetting/drying cycles compared with the NFWS of El-Shatbi Tombs. Consequently, the former (EFWS) presented more weathering (DC) reflected in a higher *Pc* (%), average percentage of micro-pores less than 5 microns, SSI value, percentage of PSD of the range 0.01–0.1 microns, TDS (25000 PPM) and EC (11.5 mmhos/cm), than the latter (NFWS; Tables 6, 7). These laboratory results regarding TDS, EC, PSD and its impact on a rock's SSI strongly confirm the validity of the modified DC scale conducted in the current study (Table 3). The higher percentage of micro-pores in the range of 0.01–0.1 microns for the EFWS (around 64%) results in more trapping of salty stagnant water (Fig. 4) reaching this rock through capillary forces (where it firstly fills the micro-pores then reaches and fills the mega-pores; Rodriguez and Doehne 1999; Ruiz et al. 2007; Rudrich et al. 2011); the NFWS has less critical micro-pores (around 42%, Table 6).

The climatic conditions prevailing at the study area are almost suitable for salt crystallization, particularly for halite salt (Sonia et al. 2014) that ranges from 39 to 41% of the total dissolved salts of the samples collected at the EFWS and NFWS (Table 2). At the same time, a salt hydration/de-hydration mechanism is also expected to occur at the study area, particularly for the sulfate salts ($CaSO_4$ salt; Sperling and Cooke 1985) that ranges from 26 to 33% of the rock's salt content for the NFWS and EFWS, respectively. Halite is well known as a hygroscopic salt that moves into and on a stone's surface based on moisture influx/solar heating, respectively (Moses and Smith 1994). On the other hand, sulfate salts are less mobile salts within a rock's pore system, i.e., from inside to outside and vice versa (Rodriguez and Doehne 1999; Ruiz et al. 2007; Rudrich et al. 2011). Consequently, a given rock might have a considerable sulfates within its pore system but doesn't appear at its weathered surface. This might be the case at the study area where chlorides exceed sulfates at the weathered surface of the NFWS and EFWS. But, as the sulfates have a deleterious impact on a rock's fabric and components (Charola and Weber 1992; Steiger and Asmussen 2008), the weathering forms recorded at El-Shatbi Tombs (Table 5) have been created, and are expected to increase as time progresses, and the rock becomes very salt and exceptionally salt-prone (Table 6).

The physical properties and quality of a given rock can be examined through the ultrasonic waves' measurements (Maria et al. 2000), where a good quality "less weathered" rock is that with high velocity of these waves (*Cp*) and elastic modulus (Ed), and low internal friction (*Qc*). Also, the isotropic rock, rock with *Cp*1/*Cp*2 = 1, is better in its physical properties than that one with value more than the right one. This an-isotropism results from primary structure in a given rock, particularly lamination, as dominating in the Oolitic limestone at the study area. Correlating the ultrasonic waves' results for the control and weathered rock samples together (Table 8) on one hand, and the ultrasonic waves' results with each of rock's SSI and TDS (Tables 6, 7) on the other hand, it can be noted that the EFWS is relatively isotropic "less weathered" compared with the NFWS although the former one is exceptionally salt-prone and the latter is very salt-prone, additionally, the former has TDS (25000 PPM) of 1.5 times as that of the later one (15000 PPM). Simply, the rock's SSI and TDS (Tables 6, 7 respectively) are highly correlated together but neither of them can be correlated with the ultrasonic wave results. The explanation is this laminated limestone with a noticeable difference in *Cp*1 and *Cp*2 of the control samples (Table 8) contains considerable halite and sulfate salts that destroy a rock's fabric and components; this occurs through a mechanism based on the prevailing climatic conditions. As such, these salts have been withdrawn at the stone's surface, particularly for the EFWS, reducing its an-isotropism by filling the rocks' pores and enabling these waves to pass in the two directions of measurement (*Cp*1 and *Cp*2). This gives a *Cp*1/*Cp*2 value close to the right one (1.11) compared with that of the NFWS that retains a sort of empty micro-pore, reducing the *Cp*2 (measured at a right angle to the lamination) and leading to a value of 1.19 for the isotropism calculation (Table 8). Regardless of the isotropism of EFWS compared with the NFWS, the former is still more damaged on both micro- and mega-scales than the latter.

Conclusions

The damage category scale created by Fitzner and Heinrichs (2002) was not specific and applicable and doesn't enable researchers to get the same DC of a given archaeological site. Consequently, this classification has been modified in the current study and has been applied for the Greco-Roman-age El-Shatbi Tombs located on the Mediterranean Sea. The bedrock through which these tombs had been excavated is pure carbonate rock of an oolitic type with a primary structure (lamination). This site is affected by sea spray and domestic water containing soluble salts, thereby affecting the rock's fabric and

creating very diagnostic features of salt weathering at the stones' surface; this leads to a very severe damage category (using the DCAW scheme and the modified DC scale) on both wall sides of this site. The TDS of the EFWS is 1.5 times as that of the NFWS; the rock's salt content on both sides of these tombs results in increasing the rock's connected porosity with reduction of pore radii to the range of 0.01–0.1 micron with 64 and 42% of the *P*c for the EFWS and NFWS, respectively. Consequently, the former is exceptionally salt-prone (with an SSI value of 17.4) and the latter is very salt-prone (with an SSI value of 13.44). Contrarily, these salts blocked the primary structure of the EFWS more than that of the NFWS, resulting in more isotropism for the former than the latter; i.e., the EFWS is more close to iso-tropism (1.11) compared with the NFWS (1.19).

Acknowledgements The authors are grateful for the constructive comments of the reviewers and the editor of BOEG, who exerted much effort in corrections of the original manuscript. Also, the authors deeply thank Prof. Dr. Derek Alex for reviewing the English of this paper. The authors would also like to thank the JSPS which offered the financial support for this research at Saitama Univ., Japan (ID no. L-12501).

References

Allison JR (1988) A non-destructive method of determining rock strength. Earth Surf Proc Land 13:729–736

Attewell PB, Taylor D (1990) Time dependent atmospheric degradation of building stone in a polluting environment. Eng Geol Water Sci 16(1):43–55

Calleja L, Montoto M, Perez B, Villar BM (2000) An Ultrasonic method to analyze the progress of weathering during cyclic salt crystallization tests. In: Proceedings of the 9th International Congress on Deterioration and Conservation of Stone, 19–24 June 2000. Amsterdam, Elsevier, pp 313–318

Charola AE, Weber J (1992) The hydration-dehydration mechanism of sodium sulfate. In: Rodrigues JD, Henriques F, Jeremias FT (eds) Proceedings of the Seventh International Congress on Deterioration and Conservation of Stone, Lisbon, pp 581–590

Dearman WR (1995) Description and classification of weathered rocks for engineering purposes: the background to the BS 5930: 1981 proposals. Quart J Eng Geol Hydrol 28:267–276

Dunham RJ (1962) Classification of carbonate rocks according to depositional, texture. In: Ham WE (ed) Classification of carbonate rocks, pp 108 – 121 (Mem. Am. Petrol. Geol. 1, Tulsa)

Fitzner B, Heinrichs K (2002) Damage diagnosis on stone monuments—weathering forms, damage categories and damage indices. Understanding and Managing stone decay, Prikryl and Viles (eds), The Karolinum Press, pp 11–56

Flatt RJ (2002) Salt damage in porous materials: how high supersaturations are generated. J Cryst Growth 242:435–454

Hall C, Hoff W (2007) Rising damp: capillary rise dynamics in walls. Proc R Soc A 463:1871–1884

Hall C, Hamilton A, Hoff DW, Viles AH, Eklund JA (2010) Moisture dynamics in walls: response to micro-environment and climate change. Proc R Soc A 2011(467):194–211

Harrison DJ, Hudson JH, Cannell B (1994) Appraisal of high purity limestone in England and Wales. British Geological Society, Part 1, pp 1–18

Kamh GME (2000) A comparative study on the impact of environmental geological conditions on some archaeological sites at Giza (Saqara region) and Alexandria governorates, and their modes of preservation. PhD, 2000, Geology Dept., Menoufiya Univ., Egypt (2000)

Kamh GME (2009a) Rate and mechanism of alveolar weathering of cement based masonry bricks and mortar in arid climate. Restor Build Monum An Int J 15(3):195–204

Kamh GME (2009b) Quantification and modeling of damage category of weathering forms of monumental rocks based on field measurements. Restor Build Monum An Int J 15(1):21–38

Kamh GME, Azzam R (2008) Field and laboratory investigations to examine the damage category of monumental sandstone in arid regions: seti I Temple, upper Egypt, a case study. Int J Restor Build Monum 14(3):179–196

Kapranos PA, Al-Helaly MH, Whittaker AVN (1981) Ultrasonic velocity measurements in 316 Austenitic Weldments. Br J Non-Destr Test 23(6):211–222

Kay EA, Fookes PG, Pollock DJ (1981) Deterioration related to chloride ingress. J Concr 15:22–28

Maria AG, Maria AV, Emilio G, Zezza F (2000) The physical-mechanical properties and ultrasonic data as criteria for evaluation of calcareous stone decay. In; Proceedings of 9th International Congress on Deterioration and Conservation of Stone, June 2000, Amsterdam, Elsevier, pp 309–312

McGreevy JP (1985) A preliminary scanning electron microscope study of honeycomb weathering of sandstone in a coastal environment. Earth Surf Proc Land 10:509–518

McGreevy BJ (1988) Contour scaling of a sandstone by salt weathering under simulated hot desert conditions. Earth Surf Proc Land 13:697–705

McGreevy BJ (1996) Pore properties of limestones as controls on salt weathering susceptibility: a case study. In: Smith BJ, Warke PA (eds) Processes of Urban Stone Decay. Donhead, London, pp 150–167

Moses CA, Smith BJ (1994) Limestone weathering in the supra-tidal zone: an example from Mallorca. Rock weathering and landform evolution, Robinson and Williams (eds.), pp 433–451

Mustoe GE (1983) Cavernous weathering in the Capitol reef desert, UTAH. Earth Surf Proc Land 8:517–526

Rhoades JD (1982) Soluble salts, methods of soil analysis, part 2: chemical and microbiological properties, agronomy monograph no. 9 (2nd edition)

Rodriguez NC, Doehne E (1999) Salt weathering: influence of evaporation rate, super saturation and crystallization pattern. Earth Surf Proc Land 24:191–209

Rudrich J, Bartelsen T, Dohrmann R, Siegesmund S (2011) Moisture expansion as a deterioration factor for sandstone used in buildings. Environ Earth Sci 63:1573–1586

Ruiz A, Mees F, Jacobs P, Navarro CR (2007) The role of saline solution properties on porous limestone salt weathering by magnesium and sodium sulphate. Environ Geol 52:269–281

Said R (1990) The geology of Egypt. Balkema, Rotterdam, p 734

Smith BJ, McGreevy JP (1983) A simulation study of salt weathering in hot deserts. Geogr Ann 65:127–133

Smith BJ, Přikryl R (2007) Diagnosing decay: the value of medical analogy in understanding the weathering of building stones. In: Přikryl R, Smith BJ (eds.) Building stone decay: from diagnosis to conservation. Geological Society London, Special Publications, vol 271, pp 1–8

Smith BJ, Magee RW, Whalley WB (1994) Breakdown pattern of Quartz sandstone in a polluted urban environment, Belfast, Northern Ireland. Rock Weathering and Landform Evolution, Robinson DA, Williams RBG (eds.) pp 131–150

Sonia G, Pel L, Klaas K (2014) Crystallization behavior of sodium chloride droplet during repeated crystallization and dissolution cycles: an NMR study. J Cryst Growth 391:64–71

Sperling CHB, Cooke RU (1985) Laboratory simulation of rock weathering by salt crystallization and hydration processes in hot arid environments. Earth Surf Proc Land 10:541–555

Steiger M, Asmussen S (2008) Crystallization of sodium sulfate phases in porous materials: the phase diagram Na_2SO_4-H_2O and the generation of stress. Geochimica Acta 72:4291–4306

Takahashi K, Suzuki T, Matsukura Y (1994) Erosion rates of a sandstone used for a masonry bridge pier in the coastal spray zone. Rock weathering and landform evolution, Robinson and Williams (eds.), pp 175–192

Thomachot S, Gommeaux M, Fronteau G, Oguchi CT, Eyssautier S, Kartheuser B (2011) A comparison of the properties and salt weathering susceptibility of natural and reconstituted stones of the Orval Abbey (Belgium). Environ Earth Sci 63:1447–1461

Török Á, Přikryl R (2010) Current methods and future trends in testing, durability analyses and provenance studies of natural stones used in historical monuments. Eng Geol 115(3–4):139–142

Turkington AV (1998) Cavernous weathering in sandstone: lessons to be learned from natural exposure. Quart J Eng Geol Hydrogeol 31:375–383 **(Turkington)**

Vendrell MS, Garcia M, Alarcon S (1996) Environmental impact on the Roman monuments of Tarragona, Spain. Environ Geol 27:263–269

Yamashita S, Suzuki T (1986) Change in pore size distribution of sedimentary rocks due to weathering and the resultant decrease in their strength. Trans Jpn Geomorph Union 7:257–273

Yu S, Oguchi CT (2010) Role of pore size distribution in salt uptake, damage, and predicting salt susceptibility of eight types of Japanese building stones. Eng Geol 115(3–4):226–236

Zehnder K, Schoch O (2009) Efflorescence of mirabilite, epsomite and gypsum traced by automated monitoring on-site. J Cult Herit 10:319–330